

Evaluation of Fatigue Crack-Growth-Rate Determination using a Crack-Opening-Displacement Technique for Crack-Length Measurement

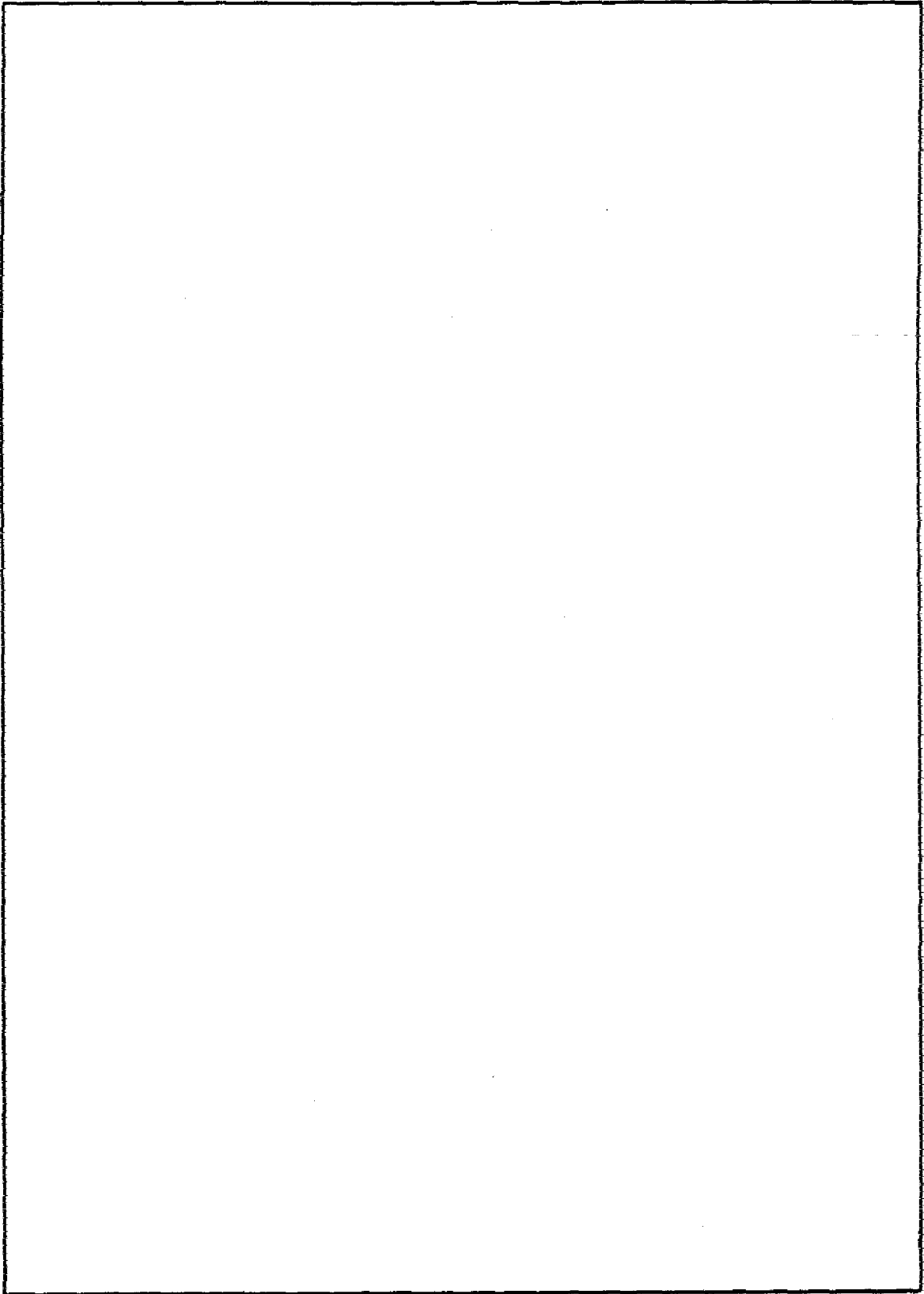
A. M. SULLIVAN AND T. W. CROOKER

*Strength of Metals Branch
Engineering Materials Division*

September 12, 1975



NAVAL RESEARCH LABORATORY
Washington, D.C.



CONTENTS

INTRODUCTION	1
EXPERIMENTAL CONSIDERATIONS	2
Material	2
Specimen Geometry	2
Test Procedure	2
Data Reduction	3
CRACK GROWTH IN 5Ni-Cr-Mo STEEL	5
CRACK GROWTH IN 10Ni STEEL	5
CRACK GROWTH IN ALUMINUM ALLOY 2024-T351	7
CONCLUSIONS	14
ACKNOWLEDGMENTS	21
REFERENCES	21
SYMBOLS	25

EVALUATION OF FATIGUE CRACK-GROWTH-RATE DETERMINATION USING A CRACK-OPENING-DISPLACEMENT TECHNIQUE FOR CRACK-LENGTH MEASUREMENT

INTRODUCTION

Rapid advances in structural technology have escalated demands for materials of greater strength so that weight allowances could be reduced. For fail-safe structures, materials of high fracture resistance are also required. The development of linear elastic fracture mechanics (LEFM) has provided the stress-intensity fracture-resistance parameters K_{Ic} and K_c which define load or crack length or both at instability or catastrophic fracture.

However, the evaluation and use of these static fracture-resistance values in design do not completely insure structural safety. Cracks grow under service conditions, and the conditions of this growth must be understood. The field of fatigue crack-growth-rate (FCGR) testing has found the stress-intensity-range parameter ΔK suitable for the assessment of crack-growth resistance under repeated loading conditions. However, no standards for such testing have been established.

An initial step to rectify this condition was taken by the ASTM Subcommittee E24.04 in conducting a Round Robin Program among 15 laboratories using various specimen types and methods of data reduction [1]. A prime source of variability was identified as crack-length determination. Optical measurement, currently the most common means of obtaining experimental crack-length data, is both time consuming and subject to operator bias. The development of a simple, reliable, and accurate means of sensing crack length using an analog technique would not only improve reliability but also further the current trend towards automation in testing.

Indirect measurement of crack length a by means of a clip gage monitoring the crack-opening displacement (COD) has been reliably employed for specimens under static loading conditions [2,3], but its application to FCGR testing has been sporadic, unstandardized, and not widely documented [4-6]. A program to develop, evaluate, and document procedures for clip-gage measurements of COD for use in FCGR testing has been recently initiated at NRL. The first phase of the program, calibration of COD to relative crack length a/W , has been completed [7].

This report discusses the application of this technique to a series of FCGR tests on several materials and evaluates its potential.

Note: Manuscript submitted June 19, 1975.

Table 1 — Nominal Composition

Material	C	Ni	Cr	Mo	V	Al	Co	Mn	P	S	Si	Mg	Cu	Fe
5Ni-Cr-Mo steel	0.11	4.85	0.58	0.48	0.07	0.018	—	0.87	0.002	0.005	0.30	—	—	Bal.
10Ni steel	0.12	10.29	2.03	1.03	—	—	8.07	0.28	0.008	0.006	0.07	—	—	Bal.
2024-T351 aluminum	—	—	—	—	—	Bal.	—	0.6	—	—	—	1.5	4.5	—

Table 2 — Mechanical Properties

Material	Yield Strength (0.2% offset) (ksi)	Tensile Strength (ksi)	Elongation (%)	Reduction of Area (%)
5Ni-Cr-Mo steel				
Longitudinal	142	152	20	68
Transverse	147	152	18	64
10Ni steel				
Longitudinal	190	197	17	69
Transverse	190	197	17	69
2024-T351 aluminum				
Longitudinal	55	68	20	—
Transverse	49	68	18	—

EXPERIMENTAL CONSIDERATIONS

Material

Two high-strength steels and an aluminum alloy were tested in this program. Details are contained in Tables 1 and 2.

Specimen Geometry

The dimensions of the CT specimen (Fig. 1) conform to those selected for the ASTM E24.04 Round Robin program [1]. However, to provide a longer fatigue crack extension beyond the machined notch, the initial notch length a_0 was reduced from 0.700 to 0.500 in. (17.5 to 12.5 mm).

Test Procedure

The specimens were cycled in tension-tension loading using the haversine function of a 110-kip-capacity MTS closed-loop testing machine. The cyclic frequency was 5 Hz, and the stress-ratio R value was 0.10. The COD measurements were made using a commercial MTS clip gage, the notched arms of which fit over knife edges screwed onto the specimen to

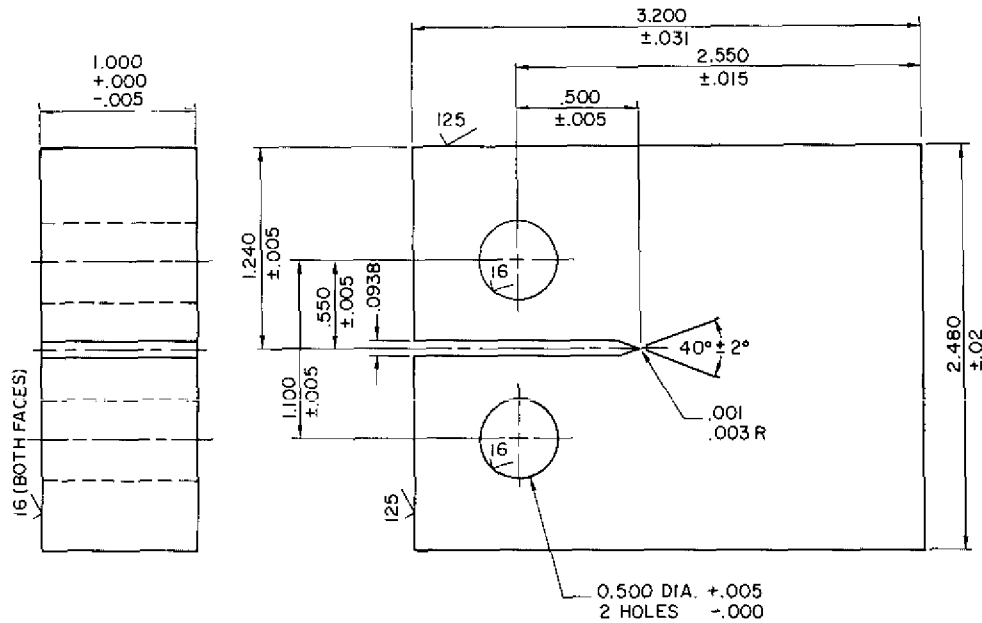


Fig. 1 — Configuration of the Compact Tension (CT) specimen recommended by ASTM Committee E24.04

straddle the mouth of the slit (Fig. 2). Signals from the strain-gage circuit were fed into a Hewlett-Packard XY recorder together with those from the load cell of the testing machine.

Loads were chosen to give predetermined ΔK values, and no discrimination in load level was made between fatigue precracking and the test itself.

Data Reduction

Crack length was determined both visually using a 15 X telescope affixed to a slide micrometer and by reference to the predetermined EB[COD]/P-vs-a/W calibration of Fig. 3. A technique for this has been described in detail elsewhere [7].

Crack growth rate was determined by fitting tangents to the a-vs-N curves using a Bausch and Lomb split-prism tangent meter.

The stress-intensity range ΔK is computed from the equation appropriate to the h/W ratio of the specimen [8] (here h/W = 0.486):

$$\Delta K = \Delta\sigma\sqrt{aY},$$

where $Y = 30.96 - 195.8(a/W) + 730.6(a/W)^2 - 1186.3(a/W)^3 + 754.6(a/W)^4$.

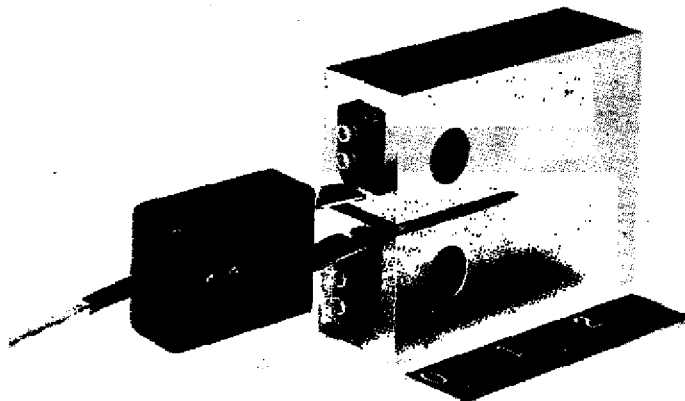


Fig. 2 — CT specimen showing the clip gage attached to the knife edges

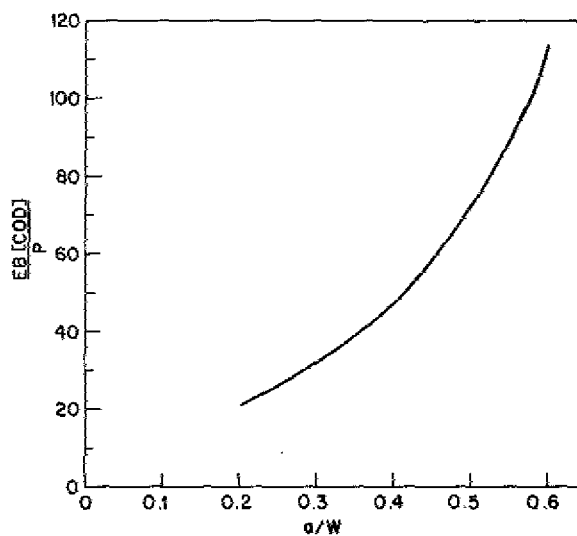


Fig. 3 — Calibration curve $EB[COD]/P$ vs a/W ; polynomial fit:

$$a/W = 0.01520 \frac{EB[COD]}{P} - 0.000141 \left(\frac{EB[COD]}{P} \right)^2 + 0.00000524 \left(\frac{EB[COD]}{P} \right)^3 - 0.06209.$$

CRACK GROWTH IN 5Ni-Cr-Mo-STEEL

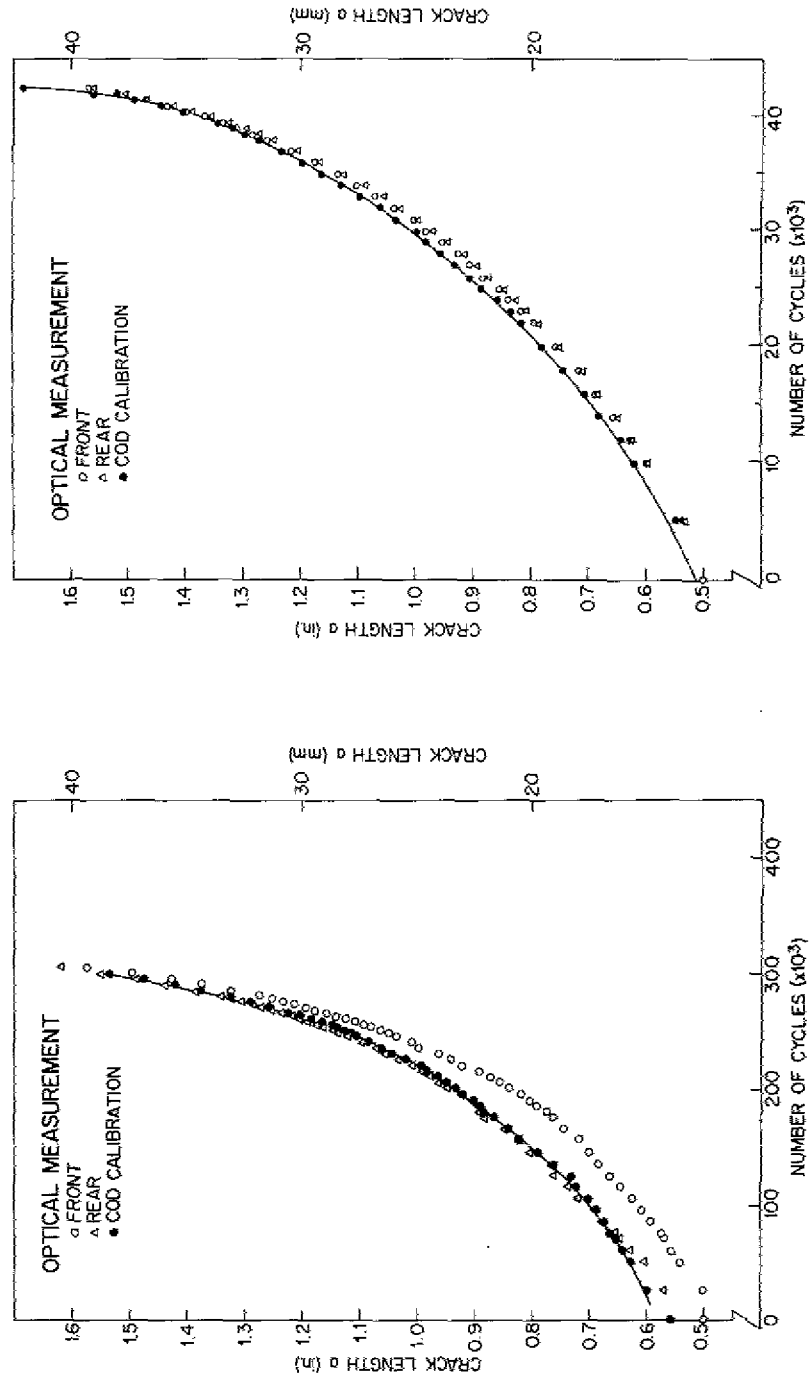
To check the accuracy of the COD calibration for determining crack length, CT test specimens were prepared from 5Ni-Cr-Mo-V high-strength steel for which crack-growth characteristics were known from a previous study [9].

Figure 4a shows crack-length values measured on the surface by a traveling optical micrometer and by reference to the COD calibration curve. It is easily seen that here there is a disparity between the optical measurements on both sides of the crack. Though slight differences might be expected, these are believed due to the fact that the crevice separation was 1 in. (25 mm), whereas the specimen thickness was 0.90 in. (22.5 mm) and no shims were used for centering. The specimen consistently shifted to abut the rear side of the specimen where the optically measured crack growth was greatest. The indirect (COD) crack measurement agreed better with the rear crack lengths in the early stages of growth. In another specimen where shims were used to center the specimen on the loading pins, the disparity between measurements on the two faces is far less noticeable (Fig. 4b).

The close agreement between the FCGR values (da/dN vs ΔK) determined from COD measurements and the previous trend line developed from both part-through crack (PTC) and center-crack tension (CCT) specimens is evident in Fig. 5. Here, although crack-length measurement is commenced at the initial notch length ($a_0 = 0.500$ in.), ΔK data are reported only after the crack has grown to 0.650 in. (16 mm) and continues to the final value of 1.525 in. (38 mm). Further details of the fatigue test parameters can be found in Tables 3 and 4. The linear portion of the log-log da/dN -vs- ΔK curve commences at a crack length of 0.800 in. (20 mm), where $a/W = 0.314$. It is noted that for the specimens tested at the higher loads, no initial "tail" is seen even at the short crack length of 0.650 in. However, this has not been found to be universally true in other materials. Experience here has indicated that disparities from linearity in the da/dN -vs- ΔK plot which are not related to the material occur when the crack length becomes greater than 1.400 in. (35 mm), where $a/W = 0.549$.

CRACK GROWTH IN 10Ni STEEL

For further comparison, CT test specimens 0.9 in. thick were prepared from the same 10Ni steel used for the recent Round Robin program on FCGR testing conducted by ASTM Subcommittee E24.04. This was made available through the courtesy of the U.S. Steel Corporation and ASTM Committee E-24. Two specimens were tested at the same load used by the ASTM Round Robin program, and two more were tested at a higher load which produced a ΔK value equivalent to the final ΔK of the first specimens; test details are contained in Tables 3 and 5. A comparison is seen in Fig. 6 between crack-length values measured by a traveling micrometer and by reference to the COD calibration. A log-log plot of da/dN vs ΔK for this material is seen in Fig. 7. Data plotted here are again for crack lengths 0.650 to 1.525 in. (16 to 38 mm). Statistical analysis of the trend line uses data for crack lengths between 0.750 and 1.400 in. (18 to 35 mm). This trend line differs slightly from that of the Round Robin program ($da/dN = 4.9 \times 10^{-9} \Delta K^{2.33}$), but the Round Robin data are over the crack-length range of 0.850 to 2.04 in. (21 to 51 mm), thus including the very high data points where scatter and nonlinearity are evident. It is also interesting to note that although this curve commences at a longer



(a) No centering shims used

(b) With centering shims

Fig. 4 — Crack length (a) vs number of cycles for 5Ni-Cr-Mo-V steel

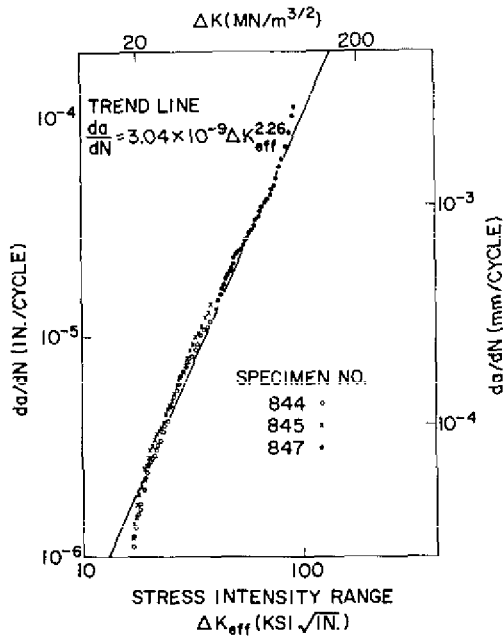


Fig. 5 — da/dN vs ΔK_{eff} for 5Ni-Cr-Mo-V steel. The trend line was previously determined from tests using other specimen geometries and optical crack-length measurement.

crack length (containing a fatigued precrack of 0.10 in. (2.5 mm)), an initial “tail” is observed. Further, the Round Robin specimens were tested in the ASTM designated LT orientation [10], whereas the NRL specimens were in the TL orientation, that is, crack growth was parallel to the rolling direction of the plate. The important observation is that calculations made using crack-length values determined by the COD technique faithfully reproduce all features of curves produced from optically measured a values. The significance of nonlinearity (“tails”) at both low and high ΔK values remains to be resolved.

CRACK GROWTH IN ALUMINUM ALLOY 2024-T351

The first specimen of this material behaved in an apparently anomalous manner (Fig. 8a). The crack grew slightly and sporadically, and then for long periods no growth was observed. Finally, growth became regular and proceeded at a constant rate until the crack had grown to a length of 1.15 in. and a ΔK value of 13.34 ksi $\sqrt{\text{in.}}$; thereafter, acceleration was observed (Fig. 8b). The second and third specimens behaved normally throughout the tests (Figs. 8c and 8d). The crack fronts were essentially straight in all cases. This is reinforced by the close agreement of optical and COD-calibration determination of crack length. Plotted as da/dN vs ΔK from the calibration-derived values (Fig. 9), a straight-line portion over the range $\Delta K = 9$ to 25 ksi $\sqrt{\text{in.}}$ can be fitted by the regression curve

$$\frac{da}{dN} = 1.71 \times 10^{-9} \Delta K_{eff}^{3.45}$$

Table 3 — Details Of Fatigue Tests

Specimen Number	σ (ksi)	a_0 (in.)	a_1 Start Data (in.)	a_2 On Straight Line (in.)	a_3 Off Straight Line (in.)
5Ni-Cr-Mo-V					
844	1.73	0.500	0.650	0.800	—
847	1.73	0.500	0.650	0.800	—
847	2.75	0.500	0.650	0.650	1.425
10Ni-Co-Cr-Mo					
848	1.73	0.500	0.650	0.750	1.400
851	1.73	0.500	0.650	0.750	1.400
849	2.75	0.500	0.650	0.750	1.400
852	2.75	0.500	0.650	0.750	1.400
2024-T351					
836	.533	0.765	0.825	1.300	—
838	.866	0.892	0.925	1.050	—
837	1.200	0.765	0.800	0.900	1.425

Estimates of crack growth from this equation are also shown on Figs. 8b and 8c from selected starting points. Test data are presented in Tables 3 and 6.

It appears that, regardless of initial load, fatigue crack growth on the order of 0.15 in. is required for the $da/dN-\Delta K$ data to fall along the common, straight-line portion of the curve; that is, precracking on the order of 0.15 in. was necessary to eliminate the lower "tail" of the curve. These data points were omitted from the statistical calculation.

When the crack-growth tests were terminated at $a/W = 0.60$ in., the specimens were fractured. Microscopic examination of the surface of the specimen tested at the lowest load showed two regimes of separation: zone 1 up to 1.15 in., which showed no fatigue striations; zone 2, which showed normal markings. These surfaces are shown in Fig. 10.

Loading for the second specimen was chosen to commence at the final ΔK value of the first specimen. Initial surface markings are virtually identical (Fig. 11).

Table 4 — 5Ni-Cr-Mo-V Steel

Specimen Number	Stress (ksi)	Crack Length a (in.)	ΔK (ksi $\sqrt{\text{in.}}$)	$\frac{da}{dN}$ 10^{-6} in./cycle
844	1.743	0.650	16.9	1.11
		0.675	17.2	1.25
		0.700	17.5	1.36
		0.725	17.8	1.56
		0.750	18.2	1.62
		0.775	18.5	1.75
		0.800	18.8	2.02
		0.825	19.3	2.29
		0.850	19.6	2.41
		0.875	20.1	2.54
		0.900	20.5	2.68
		0.925	21.0	2.82
		0.950	21.4	2.88
		0.975	21.8	3.08
		1.000	22.4	3.26
		1.025	22.8	3.38
		1.050	23.4	3.73
		1.075	23.8	3.92
		1.100	24.4	4.16
		1.125	25.0	4.90
		1.150	25.5	5.24
		1.175	26.1	5.36
		1.200	26.7	5.75
		1.225	27.3	6.18
1.250	28.0	6.51		
1.275	28.7	6.86		
1.300	29.4	7.26		
1.325	30.2	7.69		
1.350	31.0	7.92		
1.375	31.9	8.18		
1.400	32.8	8.72		
1.425	33.8	9.33		
1.450	34.8	10.10		
1.475	36.0	10.82		
1.500	37.2	11.10		
1.525	38.6	11.76		
845	1.743	0.650	16.9	1.22
		0.675	17.2	1.38
		0.700	17.5	1.50
		0.725	17.8	1.72
		0.750	18.2	1.92
		0.775	18.5	2.06
		0.800	18.8	2.26
		0.825	19.3	2.50

SULLIVAN AND CROOKER

Table 4 — (Continued)

Specimen Number	Stress (ksi)	Crack Length a (in.)	ΔK (ksi $\sqrt{\text{in.}}$)	da/dN 10^{-6} in./cycle
		0.850	19.6	2.58
		0.875	20.1	2.82
		0.900	20.5	3.08
		0.925	21.0	3.20
		0.950	21.4	3.44
		0.975	21.8	3.64
		1.000	22.4	3.74
		1.025	22.8	3.92
		1.050	23.4	4.16
		1.075	23.9	4.51
		1.100	24.4	4.74
		1.125	25.0	4.91
		1.150	25.5	5.12
		1.175	26.1	5.62
		1.200	26.7	6.04
		1.225	27.3	6.34
		1.250	28.0	6.51
		1.275	28.7	6.86
		1.300	29.4	7.47
		1.325	30.2	7.93
		1.350	31.0	8.72
		1.375	31.9	9.33
		1.400	32.8	10.02
		1.425	33.8	10.41
		1.450	34.8	11.28
		1.475	36.0	12.28
		1.500	37.2	12.86
		1.525	38.6	14.18
847	4.25	0.650	41.3	13.49
		0.675	42.0	14.53
		0.700	42.6	15.62
		0.725	43.4	16.48
		0.750	44.2	17.21
		0.775	45.1	18.65
		0.800	46.1	19.31
		0.825	47.0	20.00
		0.850	48.0	20.56
		0.875	49.0	21.82
		0.900	50.0	23.41
		0.925	51.1	24.26
		0.950	52.2	24.70
		0.975	53.3	25.14
		1.000	54.5	26.06
		1.025	55.8	27.52

Table 4 — (Continued)

Specimen Number	Stress (ksi)	Crack Length a (in.)	ΔK (ksi $\sqrt{\text{in.}}$)	da/dN 10^{-6} in./cycle
		1.050	57.0	28.56
		1.075	58.2	29.65
		1.100	59.8	30.56
		1.125	60.8	32.64
		1.150	62.2	33.95
		1.175	63.8	34.64
		1.200	65.2	37.61
		1.225	66.6	39.20
		1.250	68.4	41.00
		1.272	70.0	42.80
		1.300	71.8	44.90
		1.325	73.7	47.12
		1.350	75.6	49.51
		1.375	77.8	52.11
		1.400	80.1	59.80
		1.425	82.4	65.40
		1.450	85.0	74.60
		1.475	87.8	86.62
		1.500	90.8	102.81
		1.525	94.2	113.43

Table 5 — 10Ni Steel

Specimen Number	Stress (ksi)	Crack Length a (in.)	ΔK (ksi $\sqrt{\text{in.}}$)	da/dN 10^6 in./cycle	
				COD	Optical
848	1.743	0.650	16.9	2.14	1.75
		0.675	17.2	2.25	1.95
		0.700	17.5	2.31	2.17
		0.725	17.8	2.41	2.37
		0.750	18.2	2.54	2.50
		0.775	18.5	2.71	2.66
		0.800	18.9	2.90	2.88
		0.825	19.2	2.98	3.08
		0.850	19.6	3.08	3.20
		0.875	20.1	3.26	3.32
		0.900	20.5	3.38	3.44
		0.925	21.0	3.64	3.70
		0.950	21.4	3.85	3.92
		0.975	21.8	4.00	4.08
		1.000	22.4	4.16	4.51
		1.025	22.8	4.38	4.70
		1.050	23.4	4.74	4.99

SULLIVAN AND CROOKER

Table 5 - (Continued)

Specimen Number	Stress (ksi)	Crack Length a (in.)	ΔK (ksi $\sqrt{\text{in.}}$)	da/dN 10^6 in./cycle	
				COD	Optical
849	2.75	1.075	23.9	4.95	5.12
		1.100	24.4	5.24	—
		1.125	24.9	5.46	—
		1.150	25.5	5.88	—
		1.175	26.1	6.04	—
		1.200	26.7	6.18	—
		1.225	27.3	6.34	—
		1.250	28.1	6.91	—
		1.275	28.7	7.38	—
		1.300	29.4	7.69	—
		1.325	30.2	8.18	—
		1.350	31.0	8.72	—
		1.375	31.9	9.33	—
		1.400	32.8	10.02	—
		0.650	26.7	5.89	—
		0.675	27.2	6.70	—
		0.700	27.6	7.00	—
		0.725	28.1	7.41	—
		0.750	28.6	7.80	—
		0.775	29.2	8.10	—
		0.800	29.8	8.40	—
		0.825	30.4	8.70	—
		0.850	31.0	9.00	—
		0.875	31.6	9.21	—
		0.900	32.4	9.62	—
		0.925	33.1	10.20	—
		0.950	33.8	10.81	—
		0.975	34.5	11.11	—
		1.000	35.2	11.92	—
		1.025	36.1	12.57	—
		1.050	36.8	13.27	—
		1.075	37.7	14.02	—
		1.100	38.5	14.80	—
		1.125	39.4	15.40	—
		1.150	40.2	16.30	—
1.175	41.2	17.30	—		
1.200	42.2	18.04	—		
1.225	43.1	18.42	—		
1.250	44.2	19.00	—		
1.275	45.3	21.54	—		
1.300	46.4	22.96	—		
1.325	47.6	24.75	—		

Table 5 - (Continued)

Specimen Number	Stress (ksi)	Crack Length a (in.)	ΔK (ksi $\sqrt{\text{in.}}$)	da/dN 10 ⁶ in./cycle	
				COD	Optical
851	1.73	1.350	48.9	26.05	—
		1.375	50.3	29.04	—
		1.400	51.8	31.72	—
		0.650	16.9	1.88	—
		0.675	17.2	1.96	—
		0.700	17.5	2.37	—
		0.725	17.8	2.62	—
		0.750	18.2	2.78	—
		0.775	18.5	3.03	—
		0.800	18.9	3.22	—
		0.825	19.2	3.32	—
		0.850	19.6	3.49	—
		0.875	20.1	3.73	—
		0.900	20.5	3.88	—
		0.925	21.0	4.04	—
		0.950	21.4	4.33	—
		0.975	21.8	4.51	—
		1.000	22.4	4.70	—
		1.025	22.8	4.91	—
		1.050	23.4	5.17	—
		1.075	23.9	5.38	—
1.100	24.4	5.69	—		
1.125	24.9	5.36	—		
1.150	25.5	5.62	—		
1.175	26.1	5.88	—		
1.200	26.7	6.68	—		
1.225	27.3	7.26	—		
1.250	28.1	7.69	—		
1.275	28.7	8.18	—		
1.300	29.4	8.72	—		
1.325	30.2	9.33	—		
1.350	31.0	10.02	—		
1.375	31.9	10.41	—		
1.400	32.8	11.28	—		
852	2.75	0.650	26.7	7.00	—
		0.675	27.2	7.26	—
		0.700	27.6	7.81	—
		0.725	28.1	8.39	—
		0.750	28.6	8.69	—
		0.775	29.2	9.32	—
		0.800	29.8	9.49	—

SULLIVAN AND CROOKER

Table 5 — (Continued)

Specimen Number	Stress (ksi)	Crack Length a (in.)	ΔK (ksi $\sqrt{\text{in.}}$)	da/dN 10^6 in./cycle	
				COD	Optical
		0.825	30.4	9.72	—
		0.850	31.0	10.00	—
		0.875	31.6	10.36	—
		0.900	32.4	10.91	—
		0.925	33.1	11.11	—
		0.950	33.8	11.50	—
		0.975	34.5	12.35	—
		1.000	35.2	12.80	—
		1.025	36.1	13.27	—
		1.050	36.8	14.28	—
		1.075	37.7	14.82	—
		1.100	38.5	15.40	—
		1.125	39.4	16.64	—
		1.150	40.2	17.32	—
		1.175	41.2	18.81	—
		1.200	42.2	19.62	—
		1.225	43.1	20.50	—
		1.250	44.2	21.44	—
		1.275	45.3	22.46	—
		1.300	46.4	23.56	—
		1.325	47.6	25.38	—
		1.350	48.9	27.93	—
		1.375	50.3	29.87	—
		1.400	51.8	32.71	—

CONCLUSIONS

- Measurement of crack length using the EB[COD]-vs-a/W calibration curve in a practical and an accurate procedure for materials which produce linear load-vs-COD traces.
- Highly reproducible data were obtained which matched optical observations and established trend lines. FCGR tests using the ASTM E24.04 CT specimens can now be conducted with confidence and accuracy using an inexpensive commercial clip gage and the procedures detailed in this report.
- The technique is well adapted for automation of FCGR testing and for application to tests involving environmental chambers.

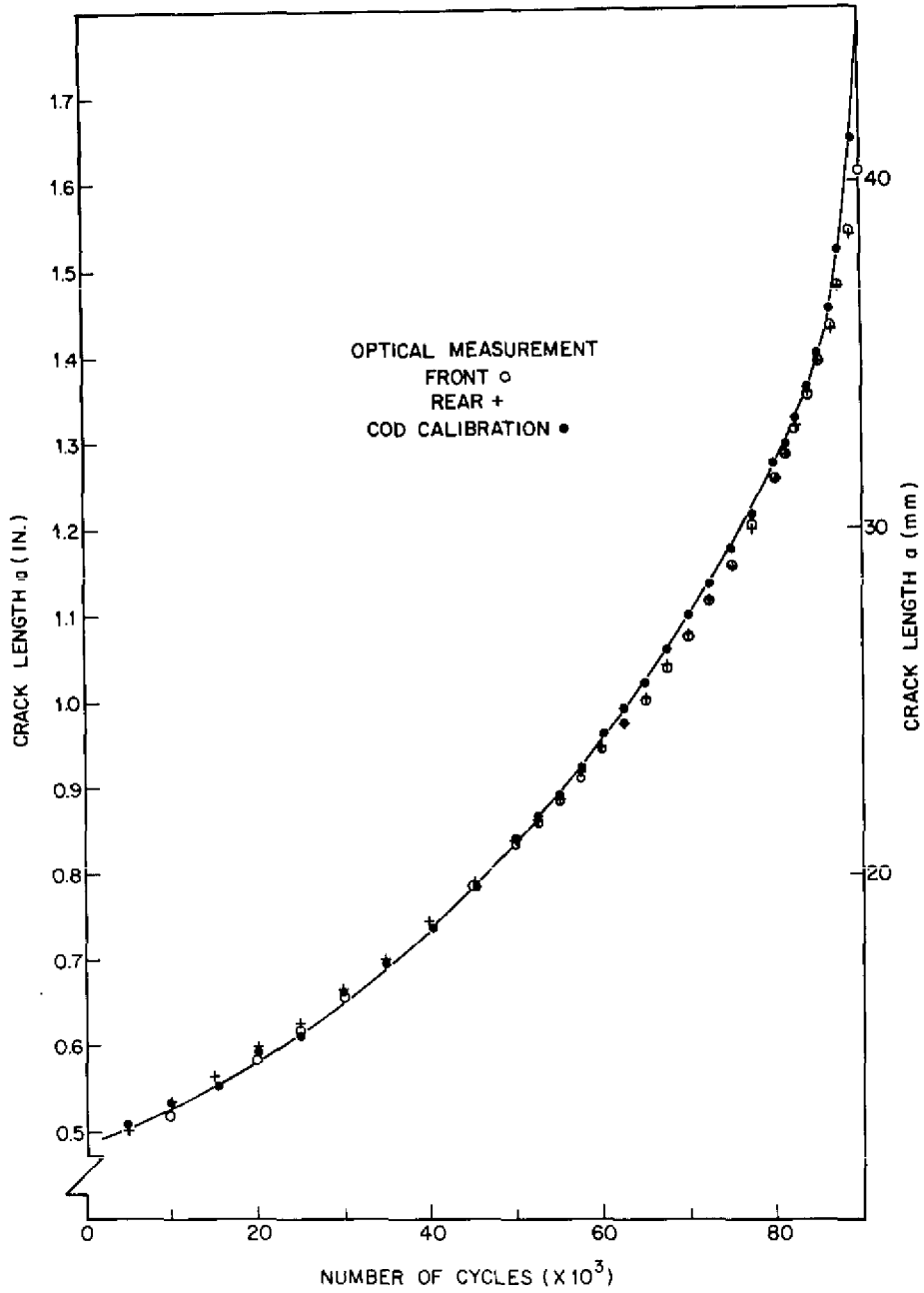


Fig. 6 - Crack length (a) vs number of cycles for 10Ni-Co-Cr-Mo steel

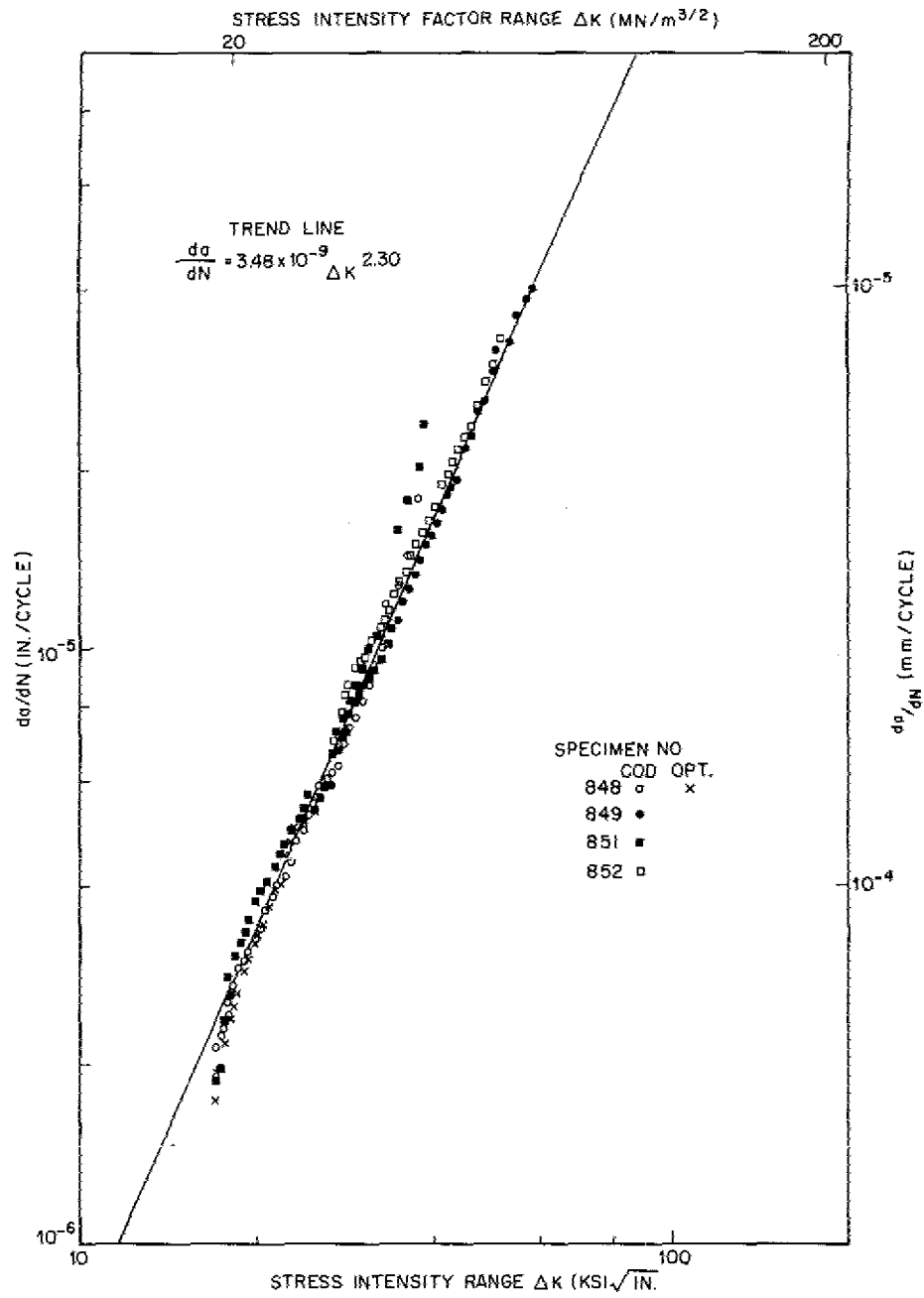
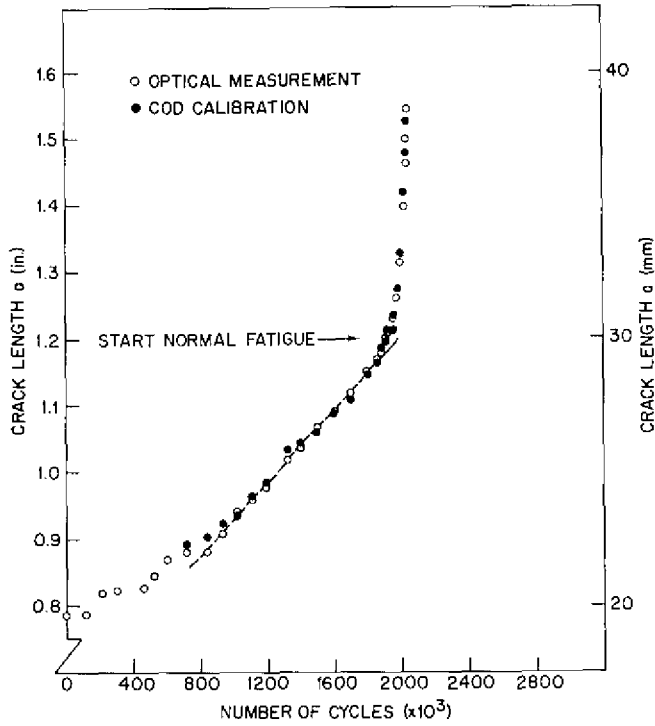
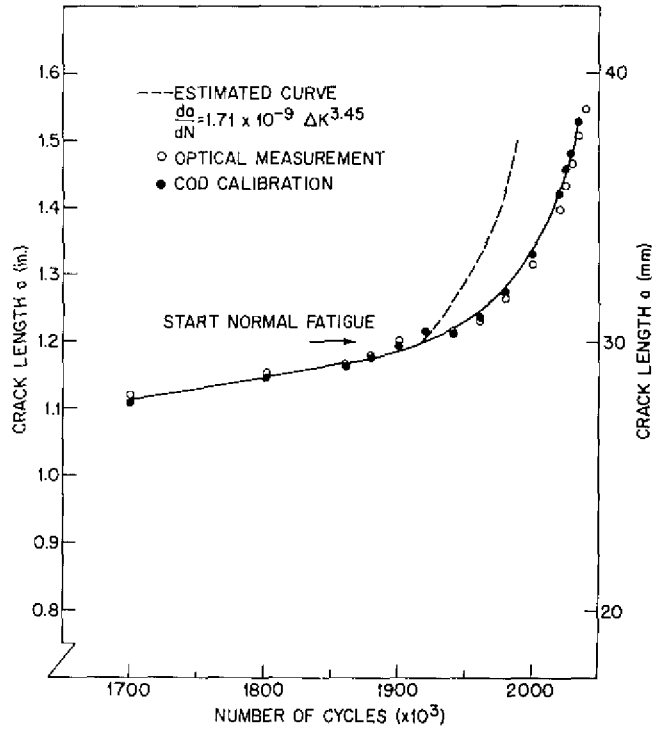


Fig. 7 — da/dN vs ΔK for 10Ni-Co-Cr-Mo steel. The trend line was computed from $a = 0.750$ to 1.400 in.



(a) Anomalous behavior at low load



(b) Accelerating portion of Fig. 8a shown on an expanded scale

Fig. 8 — Crack length (a) vs number of cycles for 2024-T351 aluminum

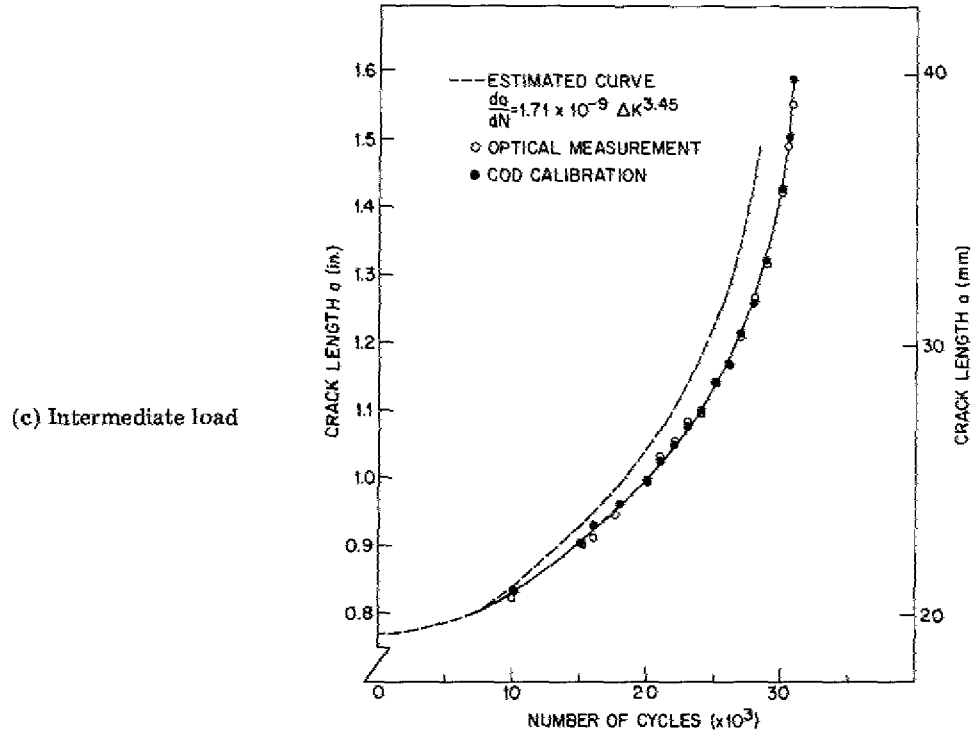
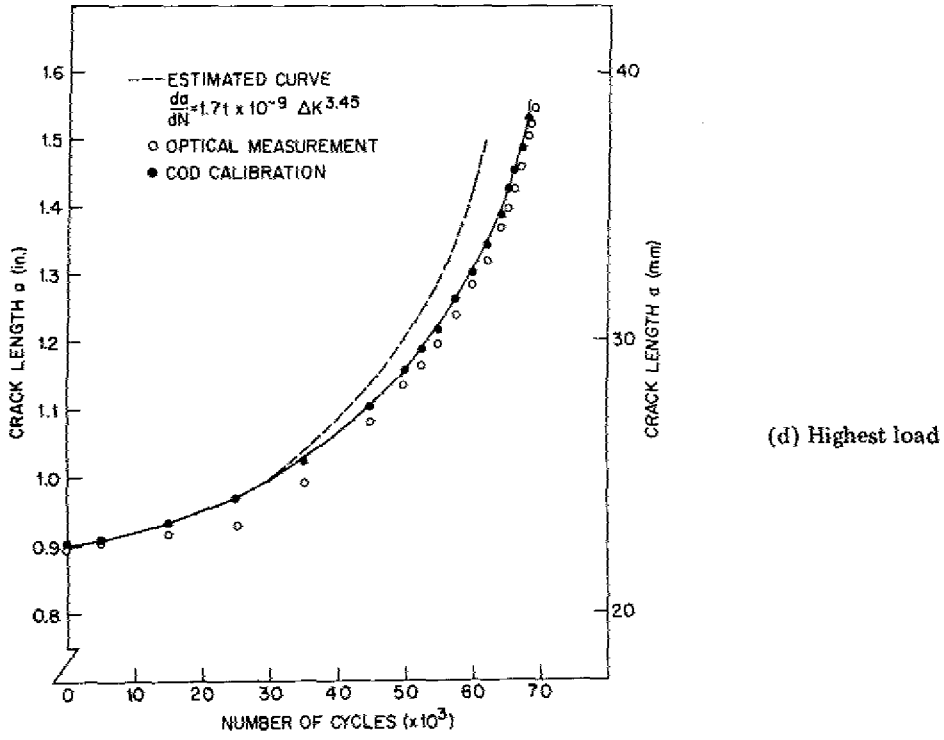


Fig. 8 - Crack length (a) vs number of cycles for 2024-T351 aluminum - Continued

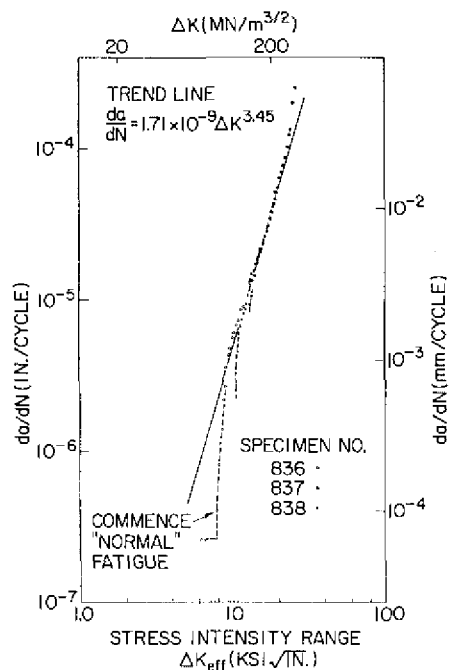


Fig. 9 — da/dN vs ΔK for 2024-T351 aluminum. Note the nonlinear portions of the dotted-line curves where $a < 0.750$ in.

Table 6 — 2024-T381 Aluminum

Specimen Number	Stress (ksi)	Crack Length a (in.)	ΔK (ksi√in.)	da/dN 10^{-6} in./cycle
836	Commence normal fatigue	0.900	6.2	0.26
		0.925	6.4	0.26
		0.950	6.5	0.26
		0.975	6.7	0.26
		1.000	6.8	0.26
		1.025	7.0	0.26
		1.050	7.1	0.26
		1.075	7.3	0.26
		1.100	7.4	0.26
		1.125	7.6	0.26
		1.150	7.8	0.26
		1.175	8.0	0.40
		1.200	8.2	0.81
		1.225	8.4	1.11
		1.250	8.8	1.38
		1.275	9.0	2.17
		1.300	9.2	2.68
1.325	9.4	3.57		
1.350	9.8	4.33		

SULLIVAN AND CROOKER

Table 6 - Continued

Specimen Number	Stress (ksi)	Crack Length a (in.)	ΔK (ksi $\sqrt{\text{in.}}$)	da/dN 10^{-6} in./cycle
837	1.20	1.375	9.8	4.80
		1.400	10.1	5.62
		1.425	10.3	6.04
		1.450	10.6	6.86
		1.475	11.0	7.40
		1.500	11.4	8.72
		1.525	11.8	9.01
		0.825	13.2	14.0
		0.850	13.5	15.3
		0.875	13.8	15.6
		0.900	14.1	18.3
		0.925	14.4	19.6
		0.950	14.7	20.4
		0.975	15.1	22.5
		1.000	15.4	24.7
		1.025	15.7	27.5
		1.050	16.1	29.3
		1.075	16.4	29.6
		1.100	16.9	31.4
		1.125	17.2	33.2
		1.150	17.6	34.6
		1.175	18.0	38.1
		1.200	18.4	39.2
		1.225	18.8	42.8
		1.250	19.2	45.8
		1.275	19.8	50.8
		1.300	20.2	55.0
		1.325	20.8	65.4
		1.350	21.3	70.6
		1.375	22.0	77.3
		1.400	22.6	107.9
		1.425	23.2	113.4
		1.450	24.0	126.2
1.475	24.8	145.4		
1.500	25.6	201.6		
1.525	26.6	254.1		
838	.86	0.925	10.4	2.5
		0.950	10.6	3.5
		0.975	10.8	4.6
		1.000	11.1	6.0
		1.025	11.4	6.7
		1.050	11.6	7.3
		1.075	11.8	8.1
		1.100	12.1	8.7

Table 6 -- (Continued)

Specimen Number	Stress (ksi)	Crack Length a (in.)	ΔK (ksi $\sqrt{\text{in.}}$)	da/dN 10^{-6} in./cycle
		1.125	12.4	9.4
		1.150	12.0	10.7
		1.175	13.0	12.8
		1.200	13.2	13.5
		1.225	13.6	14.8
		1.250	13.9	15.5
		1.275	14.2	17.2
		1.300	14.6	17.6
		1.325	15.0	19.6
		1.350	15.4	21.4
		1.375	15.8	23.6
		1.400	16.4	24.7
		1.425	16.8	29.0
		1.450	17.3	31.7
		1.475	17.8	34.8
		1.500	18.5	37.3
		1.525	19.2	51.4

ACKNOWLEDGMENTS

The authors are glad to acknowledge their colleagues, Mssrs. G. W. Jackson and M. Cigley who accepted the responsibility of running the actual tests herein discussed.

REFERENCES

- [1] W.G. Clark, Jr., and S.J. Hudak, Jr., "Variability in Fatigue Crack Growth Rate Testing (An ASTM E24.04.01 Task Group Report)," Westinghouse Research Laboratories Scientific Paper 74-1E7-MSLRA-P2, Westinghouse Research Laboratories, Pittsburgh, PA, Sept. 18, 1974.
- [2] W.F. Brown, Jr., and J.E. Srawley, "Fracture Toughness Testing," in *Fracture Toughness Testing and Its Applications* ASTM STP 381, American Society for Testing and Materials, Philadelphia, PA, 1965, p. 133.
- [3] A.M. Sullivan and C.N. Freed, "A Review of the Plane-Stress Fracture Mechanics Parameter K_c Determined Using the Center-Cracked Tension Specimen," NRL Report 7460, Dec. 1972.
- [4] R.P. Jewett, "Computer-Controlled Materials Testing for Space Shuttle Main Engine (SSME)," *Closed Loop* 4, No. 3, (1974).
- [5] T.C. Mamaros and A.T. Jones, "Using Crack-Mouth Displacement for Measurement and Control During Fracture Tests," *Closed Loop* 4, No. 4, (1974).

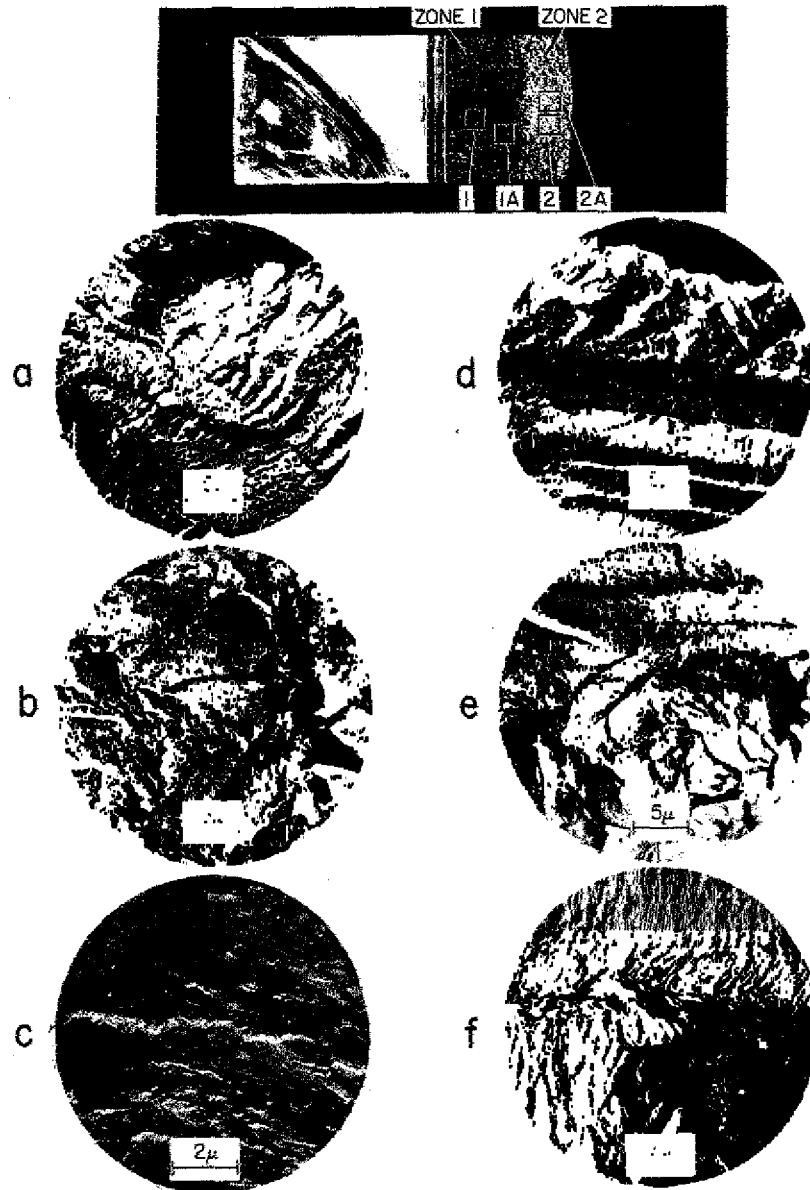


Fig. 10 — First aluminum specimen. In Zone 1, corresponding to a low, constant da/dN value (Fig. 8a), no fatigue striations are seen (a, b and c). Zone 2, where normal acceleration is observed, fatigue striations are visible (d, e, and f). Crack path is from left to right.



Fig. 11 — Second aluminum specimen. In both Zone 1 (a, b, and c) and Zone 2 (d, e, and f), fatigue striations are visible and increase in width with crack acceleration. In Zone 1, which roughly corresponds to Zone 2 of Fig. 10, fatigue striations are of approximately similar width. Crack path is from left to right.

- [6] H.I. McHenry, "A Compliance Method for Crack Growth Studies at Elevated Temperatures," *J. Materials* 6, No. 4, 862 (1971).
- [7] A.M. Sullivan, "Crack-Length Determination for the Compact Tension Specimen Using a Crack-Opening-Displacement Technique," NRL Report 7888, June, 1975.
- [8] E.T. Wessel, "State of the Art of the WOL Specimen for K_{Ic} Fracture Toughness Testing," *Engineering Fracture Mechanics* 1, 77 (1968).
- [9] A.M. Sullivan and T.W. Crooker, "Analysis of Fatigue-Crack Growth in a High Strength Steel — I. Stress Level and Stress Ratio Effects at Constant Amplitude," pending publication by ASME.
- [10] R.J. Goode, "Identification of Fracture Plane Orientation," *Materials Research and Standards* 12, No. 9, 31 (1972).

SYMBOLS

a	Crack length
a_0	Initial crack length
a/W	Crack length-to-width ratio
da/dN	Crack growth rate; change in length per cycle
B	Specimen thickness
CCT	Center-crack tension specimen
COD	Crack-opening displacement
CT	Compact tension specimen
h	Specimen half height
E	Young's modulus
FCGR	Fatigue crack-growth rate
Hz	Hertz; cycles per second
K_c	Stress-intensity parameter for plane stress
K_{Ic}	Stress-intensity parameter for plane strain
ΔK	Stress-intensity-parameter range ($K_{max} - K_{min}$)
ΔK_{eff}	Effective ΔK using a correction for the effect of stress ratio R
LEFM	Linear elastic fracture mechanics
P	Load
PTC	Part-through crack specimen
N	Number of cycles
R	Stress ratio ($\sigma_{min}/\sigma_{max}$)
W	Specimen width
σ	Stress
$\Delta\sigma$	Stress range ($\sigma_{max} - \sigma_{min}$)